AD-A128 261 AN ANALYSIS OF A FINITE ELEMENT METHOD FOR CONVECTION-DIFFUSION PROBLEMS..(U) MARYLAND UNIV COLLEGE PARK LAB FOR NUMERICAL ANALYSIS

1/1

UNCLASSIFIED W G SZYMCZAK ET AL. MAR 83 BN-1002 F/G 12/1 NL

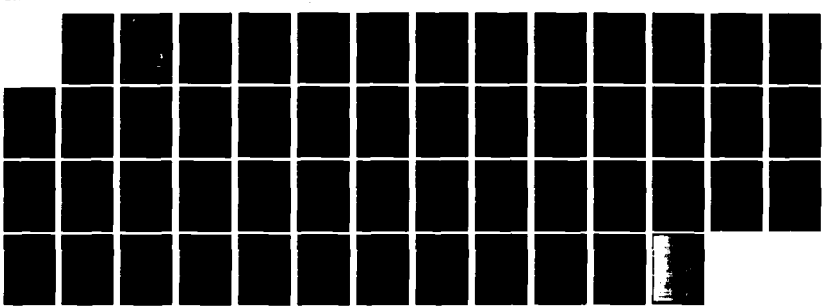

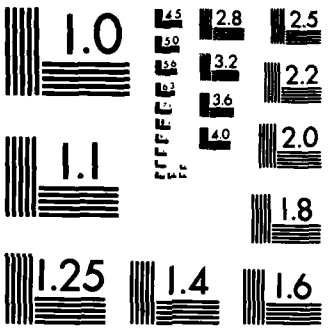

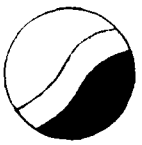

INSTITUTE FOR PHYSICAL SCIENCE AND TECHNOLOGY

Laboratory for Numerical Analysis

Technical Note BN-1002

AN ANALYSIS OF A FINITE ELEMENT METHOD FOR CONVECTION-DIFFUSION PROBLEMS

PART II: A POSTERIORI ERROR ESTIMATES AND ADAPTIVITY

by

W. G. Szymczak

and

I. Babuška

March 1983

UNIVERSITY OF MARYLAND

SECURITY CLASSIFICATION OF THIS PAGE (When Data Entered)

REPORT DOCUMENTATION PAGE

READ INSTRUCTIONS BEFORE COMPLETING FORM

1. REPORT NUMBER: Technical Report BN-1002

2. GOVT ACCESSION NO.

3. RECIPIENT'S CATALOG NUMBER

4. TITLE (and Subtitle): AN ANALYSIS OF A FINITE ELEMENT METHOD FOR CONVECTION-DIFFUSION PROBLEMS. Part II: A POSTERIORI ERROR ESTIMATES AND ADAPTIVITY

5. TYPE OF REPORT & PERIOD COVERED: final life of the contract

6. PERFORMING ORG. REPORT NUMBER

7. AUTHOR(s): W. G. Szymczak and I. Babuška

8. CONTRACT OR GRANT NUMBER(s): ONR N00014-77-0623

9. PERFORMING ORGANIZATION NAME AND ADDRESS:
Institute for Physical Science & Technology
University of Maryland
College Park, MD 20742

10. PROGRAM ELEMENT, PROJECT, TASK AREA & WORK UNIT NUMBERS

11. CONTROLLING OFFICE NAME AND ADDRESS:
Department of the Navy
Office of Naval Research
Arlington, VA 22217

12. REPORT DATE: March 1983

13. NUMBER OF PAGES: 34

14. MONITORING AGENCY NAME & ADDRESS (if different from Controlling Office)

15. SECURITY CLASS. (of this report)

15a. DECLASSIFICATION/DOWNGRADING SCHEDULE

16. DISTRIBUTION STATEMENT (of this Report)

Approved for public release: distribution unlimited

17. DISTRIBUTION STATEMENT (of the abstract entered in Block 20, if different from Report)

18. SUPPLEMENTARY NOTES

19. KEY WORDS (Continue on reverse side if necessary and identify by block number)

20. ABSTRACT (Continue on reverse side if necessary and identify by block number)

A posteriori error estimates are derived for the finite element method presented in Part I. These estimates are proven to have the property that the effectivity index θ = (error estimate/true error) converges to one as the maximum mesh size goes to zero. An adaptive mesh refinement strategy is based on equilibriating local error indicators whose sum comprises the global error estimate. Numerical results show that θ is nearly one even on coarse meshes, and that optimal meshes are created by the adaptive procedure. The successful solution of a non linear problem-modeling flow through an expanding duct, makes evident the robustness of the method.

DD FORM 1 JAN 73 1473 EDITION OF 1 NOV 65 IS OBSOLETE

S/N 0102-LF-014-6601

SECURITY CLASSIFICATION OF THIS PAGE (When Data Entered)

An Analysis of a Finite Element Method for Convection-Diffusion Problems. Part II: A Posteriori Error Estimates and Adaptivity*

W. G. Szymczak+ and I. Babuška#

Laboratory for Numerical Analysis

Technical Note BN-1002

+Applied Mathematics Branch, Code R44, Naval Surface Weapons Center, White Oak, Silver Spring, Maryland 20910.

#Institute for Physical Science and Technology, University of Maryland, College Park, Maryland 20742.

*This work was supported in part by the Office of Naval Research under contracts N00014-77-C0623 and N00014-83-WR30147.

Abstract

A posteriori error estimates are derived for the finite element method presented in Part I. These estimates are proven to have the property that the effectivity index θ = (error estimate/true error) converges to one as the maximum mesh size goes to zero. An adaptive mesh refinement strategy is based on equilibriating local error indicators whose sum comprises the global error estimate. Numerical results show that θ is nearly one even on coarse meshes, and that optimal meshes are created by the adaptive procedure. The successful solution of a non linear problem-modelling flow through an expanding duct, makes evident the robustness of the method.

CHAPTER 1

INTRODUCTION

This paper is the second part of a two part series in which an adaptive finite element method for convection diffusion problems is derived and analyzed. In the first paper an upwinded finite element method was described which was shown to yield a quasi-optimal approximation to the exact solution of the model problem

$$
\begin{aligned}
&-\varepsilon u'' + a(x)u' + b(x)u = f \quad \text{in } (0,1) \\
&u(0) = \alpha \qquad (1.1) \\
&\beta_1 u'(1) + \beta_2 u(1) = \beta.
\end{aligned}
$$

Although quasi-optimality is mathematically important, the goal of a numerical computation is to provide an accurate approximation to the exact solution of a mathematical model describing some physical phenomena. Therefore, a numerical computation should not only produce an approximate solution, but also an estimation of its accuracy.

The effectiveness of such an error estimate can be measured by the effectivity index

$$\theta = (\text{error estimate}/\text{true error}).$$

Using the upwinded finite element method described in Part I to solve (1.1), an a posteriori estimator is found such that $\theta \to 1$ as the maximum mesh spacing $h = h(\Delta) \to 0$. An error estimator with this property is called asymptotically exact. Computationally, the value of $|1 - \theta|$ is shown to be small, often less than .2, even on coarse meshes.

These estimates are derived by first considering a projection of the true error onto a space of functions which is zero at the nodes. This projected error is shown to be close to the true error in norm. Since the projected error is zero at the nodes it can be approximated locally. Therefore, each interval has a local error indicator associated with it, and the global error estimate is simply a sum of these indicators.

The error indicators lead to a procedure for adaptive mesh refinement. It has been shown by Babuška and Rheinboldt [1], [3] that the equilibriation of the error indicators leads to an optimal mesh. A strategy based on this face has been developed and described in [2], [4], [5]. That strategy is used in this paper as well.

This refinement strategy is completely automated by the computer. First, an initial solution is obtained on an unrefined mesh. Error indicators are calculated for each element and an error estimate is computed by summing the indicators. If the estimate is below some prescribed tolerance, the algorithm stops. Otherwise, a threshold value is computed and all elements having indicators above this threshold are subdivided. The algorithm continues in this way until either the specified tolerance is attained or computer resources are used up. Numerical results show this algorithm to be very effective in resolving boundary layers or other singularities in the solution.

An adaptive procedure based on a posteriori error estimates has been developed by Reinhardt ([13], [14]) for a norm which arises from symmetrizing the bilinear form. The method of symmetrization was first studied by Barrett and Morton in [6] and [7]. Unfortunately, for problems of the form (1.1) with $b(x) \neq 0$, the method described by Reinhardt requires the solution of a full matrix equation, instead of the usual band matrix for the conventional or upwinded methods.

In Chapter 2 of this paper we summarize the results from Part I. This provides the mathematical framework for the problem. The a posteriori estimates are derived in Chapter 3 and are proven to be asymptotically exact. Finally, some numerical results are presented in Chapter 4. The examples were selected in order to show the optimality of the method, the reliability of the error estimates, and the robustness of the algorithm. The robustness is displayed through the successful solution of a non-linear problem with a turning point. This problem arises from a model of flow through an expanding duct.

The asymptotic theory presented in this paper is based on the assumption that the maximum mesh size h is small. In the adaptive mode, this is not quaranteed. Ratios of the maximum step size to the minimum step size often exceeded 250 in the numerical experiments of Chapter 4. This suggests that this requirement is not necessary in practice.

Numerical results for a simple 2-D problem in which the flow is in the direction of the x-axis have been performed (with a posteriori estimates and adaptivity) and appear very promising. These results as well as further 1-D examples are in preparation.

CHAPTEP 2

PRELIMINARY RESULTS

In this chapter we summarize the results of [19] which are needed in this paper. The following notations are used:

$H_p^k(I)$, $k = 0,1,\ldots,$ $1 \le p \le \infty$ is the usual Sobolev space on the interval $I = [0,1]$ consisting of functions with k derivatives in $L_p(I)$.

$\Delta = \{0 = x_o < x_1, < \ldots < x_N = 1\}$, where $N = N(\Delta)$ is an arbitrary mesh on I.

$h_j = x_j - x_{j-1}$ and $I_j = (x_{j-1}, x_j)$ for $j = 1,\ldots, N$. $\rho_j = (h_j + h_{j+1})/2$ for $j = 1,\ldots, N-1$, $\rho_N = h_N$ and $h = \max_j h_j$

A variational setting will be presented for the problem

$$
\begin{aligned}
Lu &\equiv -\varepsilon u'' + a(x)u' + b(x)u = f \text{ in } I, \\
u(0) &= \alpha, \\
\Gamma(u) &\equiv \beta_1 u'(1) + \beta_2 u(1) = \beta.
\end{aligned} \tag{2.1}
$$

For the operator L we assume

A1: $a(x) \in C^1[0,1]$, $a(x) \ge \underline{a} > 0$,

$b(x) \in C^0[0,1]$, $b(x) \ge \underline{b}$,

and $\underline{b}$ is such that $\underline{a}^2 + 4\varepsilon\underline{b} = \gamma > 0$.

For the boundary operator Γ we assume

A2: $\beta_1, \beta_2 \ge 0$, $\beta_1 + \beta_2 > 0$.

The assumptions A1 and A2 are sufficient to ensure that a maximum principle for (2.1) holds, and the Green's function for L is bounded uniformly by a constant independently of ε.

We also have additional assumptions on the input data, namely,

A3 i) The source term f is of the form $f = f_o + f_1$, where $f_o \in L_1(I)$ and $f_1 = \sum_{i=1}^{N-1} C_i \delta(x - x_i)$, where $\delta(x - x_i)$ is the Dirac delta function at the meshpoint $x = x_i$. Furthermore, $\sum_{i=1}^{N-1} |C_i| = K$ is independent of N and f is independent of ε.

ii) α is bounded independently of ε. Also, if $\beta_1 \neq 0$ then $\frac{\varepsilon\beta}{\beta_1}$ is bounded independently of ε and if $\beta_1 = 0$ then $\frac{\beta_1}{\beta_2}$ is bounded independently of ε.

A4 $a(x)/_{I_j} \in C^{r+2}(I_j)$, $b(x)/_{I_j} \in C^{r+1}(I_j)$, $f_o(x)/_{I_j} \in C^{r+1}(I_j)$ (r will be specified later), and $a(x)$ and $b(x)$ are independent of ε.

In [19] Chapter 2 it was shown that assumptions A1-A3 are sufficient to ensure the existence of a unique solution to (2.1) which is bounded independently of ε. Assumptions A1-A4 are assumed to hold throughout this paper. Furthermore, without loss of generality, we restrict ourselves to the case of homogeneous essential boundary conditions, i.e. $\alpha = 0$, and if $\beta_1 = 0$ then $\beta = 0$. This restriction is made for the theory only, and not for the numerical examples presented. Because the Green's function is bounded it follows that if A3 holds then the solution to (2.1) is bounded independently of ε. The assumptions A1-A4 are assumed to hold throughout this paper.

Let L^* denote the formal adjoint operator to L, i.e.,

$$L^* \equiv -\varepsilon \frac{d^2}{dx^2} - a(x) \frac{d}{dx} + (b-a')(x).$$

The boundary operator adjoint to Γ is Γ^*, where for u sufficiently smooth

$$\Gamma^* u = \begin{cases} \left[\varepsilon \dfrac{\beta_2}{\beta_1} + a(1) \right] u(1) + \varepsilon u'(1), & \text{if } \beta_1 \neq 0, \\ u(1), & \text{if } \beta_1 = 0. \end{cases}$$

We now define the spaces and bilinear form used to pose (2.1) variationally. The space $H^o_{p,\Delta}$, $1 \leq p \leq \infty$ is defined as the completion of

$$H_1 = \left\{ u \in H^1_p(I): \quad u(0) = 0, \quad u(1) = 0 \quad \text{if } \beta_1 = 0 \right\},$$

with respect to the norm

$$(2.2) \qquad ||u||_{H^o_{p,\Delta}} = \begin{cases} \left[\int_0^1 |u|^p dx + \sum_{j=1}^{N_1} \rho_j |u(x_j)|^p \right]^{1/p}, & 1 \leq p < \infty, \\ ||u||_{L_\infty(I)}, & p = \infty, \end{cases}$$

where $N_1 = N - 1$ if $\beta_1 = 0$ and $N_1 = N$ if $\beta_1 \neq 0$.

The space $H^o_{p,\Delta}$ can be easily identified with $L_p \oplus R^{N_1}$, that is, $u = (\tilde{u}, d_1, \ldots, d_{N_1}) \in H^o_{p,\Delta} = L_p \oplus R^{N_1}$, and

$$(2.3) \qquad ||u||_{H^o_{p,\Delta}} = \begin{cases} \left[||\tilde{u}||^p_{L_p(I)} + \sum_{j=1}^{N_1} \rho_j |d_j|^p \right]^{1/p}, & 1 \leq p < \infty, \\ \max_j \left[||\tilde{u}||_{L_\infty(I_j)}, \ |d_j| \right], & p = \infty. \end{cases}$$

In consistency with our definition, we say $u \in H^o_{p,\Delta} \cap H^1_p(I)$ if $\tilde{u} \in H^1_p(I)$ and $d_j = \tilde{u}(x_j)$ for $j = 1, \ldots, N_1$.

The space $H^2_{q,\varepsilon,\Delta}$ is defined by $H^2_{q,\varepsilon,\Delta} = \{v \in H^1_q(I): v(0) = 0, v(1) = 0 \text{ if } \beta_1 = 0$ and $v|_{I_j} \in H^2_q(I_j)$, $j = 1, \ldots, N\}$ for $1 \leq q \leq \infty$.

For any $v \in H^2_{q,\varepsilon,\Delta}$ define $||\cdot||_{H^2_{q,\varepsilon,\Delta}}$ by

$$(2.4)\qquad ||v||_{H^2_{q,\varepsilon,\Delta}} = \begin{cases} \left[\sum_{j=1}^{N} \int_{I_j} |L^*v|^q dx + \sum_{j=1}^{N-1} \varepsilon^q |J(v'(x_j))|^q h_j^{1-q} + h_N^{1-q} |\Gamma^*(v)|^q \right]^{1/q}, & q < \infty, \\ \max\left[\max_{1\le j\le N} ||L^*v||_{L_\infty(I_j)}, \max_{1\le j\le N-1} \varepsilon |J(v'(x_j))| h_j^{-1}, |\Gamma^*(v)| h_N^{-1} \right], & q = \infty. \end{cases}$$

On $H^o_{p,\Delta} \times H^2_{q,\Delta}$, where $\frac{1}{p} + \frac{1}{q} = 1$, $1 \le p \le \infty$, we define a bilinear form $B_\Delta(\cdot,\cdot)$ by

$$(2.5)\qquad B_\Delta(u,v) = \sum_{j=1}^{N} \int_{I_j} \tilde{u} L^* v dx - \sum_{j=1}^{N-1} \varepsilon d_j J(v'(x_j)) + d_N \Gamma^*(v),$$

where $J(v'(x_j)) = v'(x_j+0) - v'(x_j-0)$ for $1 \le j \le N-1$, and $v'(x_j \pm 0) = \lim_{x \to x_j^{\pm}} v'(x)$.

The following results were proven in [19]

Lemma 2.1. (See [19] Lemma 2.6). Let $v \in H^2_{q,\varepsilon,\Delta}$, then

$$||v||_{H^2_{q,\varepsilon,\Delta}} = \sup_{u \in H^o_{p,\Delta}} \frac{|B_\Delta(u,v)|}{||u||_{H^o_{p,\Delta}}}.$$

Theorem 2.2. (See [19] Theorem 2.8). If $v \in H^2_{q,\varepsilon,\Delta}$, then $v \in L_\infty(I) \cap H^1_q(I)$ with

$$(2.6)\qquad ||v||_{L_\infty(I)} \le C_1 ||v||_{H^2_{1,\varepsilon,\Delta}} \le C_1 ||v||_{H^2_{q,\varepsilon,\Delta}}, \quad 1 \le q \le \infty,$$

and

$$(2.7) \qquad \|v'\|_{L_q(I)} \le C_2 \varepsilon^{1/q-1} \|v\|^2_{H^2_{q,\varepsilon,\Delta}}, \qquad 1 \le q \le \infty,$$

where C_1 and C_2 are independent of v, q, ε and Δ.

For the finite dimensional trial space, from which the approximation is taken, we use $S_r = \{u \in C^0 \cap H^0_{p,\Delta} : u|_{I_j}$ is a polynomial of degree $\le r\}$. For the test space, two possibilities are considered. First, consider

$$S_L^{(\eta)} = \text{Span} \left\{ \psi^{(\eta)}_{\ell,j} \right\} \quad j=1,\ldots,N_1, \quad \ell=-1,\ldots,r-2$$

where

$$(2.8a) \qquad L^*\psi^{(\eta)}_{-1,j} = \begin{cases} \eta_{-1,j}(x), & \text{on } I_j \text{ and } I_{j+1} \\ 0, & \text{elsewhere,} \end{cases}$$

$$\psi^{(\eta)}_{-1,j}(x_i) = \delta_{i,j}, \qquad \text{for } i,j = 1,\ldots,N.$$

$$(2.8b) \qquad L^*\psi^{(\eta)}_{\ell,j} = \begin{cases} \left(\frac{x-x_{j-1}}{h_j}\right)^{\ell} + \eta_{\ell,j}(x), & \text{on } I_j, \\ 0, & \text{elsewhere,} \end{cases}$$

$$\psi^{(\eta)}_{\ell,j}(x_i) = 0, \quad \text{for } \ell = 0,\ldots,r-2, \; i,j = 1,\ldots,N.$$

Let $\eta_j = \max_{\ell=-1,\ldots,r-2} \|\eta_{\ell,j}(x)\|_{L_\infty(I_j)}$, and $\eta = \max_j \eta_j$.

The following result guarentees that the finite element approximation $u_L \in S_r$ obtained when $S_L^{(\eta)}$ is the test space is quasi-optimal in $H^0_{p,\Delta}$ if η is sufficiently small.

Theorem 2.3 Let η be sufficiently small and $\frac{1}{p} + \frac{1}{q} = 1$. Then there exists a $D_o > 0$ bounded away from zero independently of ε, such that

$$\inf_{v \in S_L^{(\eta)}} \sup_{u \in S_r} |B_\Delta(u,v)| \geq D_o \ , \text{ for } 1 \leq p \leq \infty \ .$$

$$||v||_{H^2_{q,\varepsilon,\Delta}} = 1 \quad ||u||_{H^o_{p,\Delta}} = 1$$

It is shown in [19] Chapter 4 that the functions $\psi_{\ell,j}^{(\eta)}$ can be found explicitly such that $\eta_j \leq Ch_j$. Because these functions are of the form $P_1(y) + P_2(y)e^{-\lambda y}$ with $\lambda = \frac{a_o h}{\varepsilon}$, when λ is large special quadrature rules are needed to control the quadrature errors. In order to avoid this, the space $S_L^{(\eta)}$ is projected onto

$$(2.9) \quad S_\alpha^{(k)} = \text{Span} \left\{ \chi_{\ell,j} \right\} \ j=1, \ \ldots, \ N_1; \ \ell=-1, \ \ldots, \ r-2$$

where

$$\chi'_{\ell,j} = P_k((\psi_{\ell,j}^{(\eta)})') = \sum_{i=0}^{k} \alpha_i^{(\ell,j)} \phi_i \ ,$$

with P_k denoting the L_2 projection operator onto the first $k + 1$ Legendre polynomials $\phi_o, \ldots, \phi_k$ on each interval I_j. The following results holds when $S_\alpha^{(k)}$ is the test space.

Theorem 2.4. Let $S_\alpha^{(k)}$ be defined in (2.9) with $k = 2r + 1$. For $v \in H^2_{q,\varepsilon,\Delta}$ and $f \in (H^2_{q,\varepsilon,\Delta})'$ satisfying A3, define

$$F(v) \equiv \langle f,v \rangle - \begin{cases} 0 & \text{if } \beta_1 = 0, \\ \frac{\varepsilon\beta}{\beta_1} v(1) & \text{if } \beta_1 \neq 0, \end{cases}$$

Then the following hold: (See [19] Chapter 2 for a, and Theorems 3.3 and 5.3 for b, c, and d).

a) There is a unique solution $u \in H^o_{p,\Delta}$, to $B_\Delta(u,v) = F(v)$ for each $v \in H^2_{q,\varepsilon,\Delta}$, $1 < q < \infty$, $\frac{1}{p} + \frac{1}{q} = 1$, and $u \in H^o_{\infty,\Delta}$.

b) There exists an h_o, independent of ε such that for all $h \leq h_o$, there exists a unique $u_\alpha \in S_r$ satisfying

$$B_\Delta(u_\alpha, v_\alpha) = F(v_\alpha) \quad \text{for each } v_\alpha \in S_\alpha^{(k)} ,$$

and a unique $u_L \in S_r$ satisfying

$$B_\Delta(u_L, v_L) = F(v_L) \quad \text{for each } v_L \in S_L^{(\eta)} .$$

c) $$||u - u_L||_{H^o_{p,\Delta}} \leq C \inf_{w \in S_r} ||u - w||_{H^o_{p,\Delta}} , \quad 1 \leq p \leq \infty.$$

d) $$||u_L - u_\alpha||_{H^o_{p,\Delta}} \leq C \max_j h_j^{r+2} \{||f^{(r+2)}||_{L_\infty(I_j)} + ||a^{(r+2)}||_{L_\infty(I_j)} + ||b^{(r+1)}||_{L_\infty(I_j)}\}$$

for $1 \leq p \leq \infty$, and $r \geq 1$.

For the computations performed the spaces S_1 and $S_\alpha^{(3)}$ were used as the trial and test spaces. With these spaces, Theorem 2.4 yields

$$(2.10) \quad ||u - u_\alpha||_{H^o_{p,\Delta}} \leq C \inf_{w \in S_1} ||u - w||_{H^o_{p,\Delta}} + \max_j C_j h_j^3$$

where u_α is the piecewise linear finite element solution.

Numerical quadrature was performed by taking the piecewise cubic interpolant of a(x) and piecewise quadratic interpolants of b(x) and f(x), and then integrating exactly. Using this quadrature rule the finite element solution $u_h \in S_1$ exists for h sufficiently small, and the estimate (2.10) holds with u_α replaced by u_h. The details of this result are omitted here but are proven in [18] for the general case using S_r as the trial space $r \geq 1$.

CHAPTER 3

ASYMPTOTICALLY EXACT ERROR ESTIMATORS

Let

$$(3.1)\quad K^1_{B,p,\Delta} = \{u = (\tilde{u}, d_1, \ldots, d_N) \in H^o_{p,\Delta} : d_i = 0,\ i = 1,\ldots,N\},$$

and

$$(3.2)\quad K^2_{B,q,\Delta} = \{v \in H^2_{q,\varepsilon,\Delta} : v(x_j) = 0,\quad j = 1,\ldots,N\},$$

with $1 \le p,q \le \infty$, and $\frac{1}{p} + \frac{1}{q} = 1$. These spaces are denoted by the subscript B to represent the "bubble"-like characteristic of functions which vanish at each nodal point.

First, we consider an approximation to $e = u - u_L$, where $u_L \in S_r$ is the finite element solution obtained using the test space $S_L^{(\eta)}$, with η sufficiently small. Denote by Pe the solution of

$$(3.3)\qquad L(Pe) = L(e) = f - L(u_L) \quad \text{in } I_j,$$

$$Pe(x_{j-1}) = Pe(x_j) = 0, \qquad j = 1,\ldots,N.$$

Then Pe also solves the variational problem: find $Pe \in K^1_{B,p,\Delta}$, such that

$$(3.4)\quad B_\Delta(Pe,v) = B_\Delta(e,v) \quad \text{for each } v \in K^2_{B,q,\Delta},\ 1 < q < \infty.$$

Because of assumption A4, $Pe \in H^o_{\infty,\Delta}$ and is bounded independently of ε. The following result shows that $u_L + Pe$ is a superconvergent improvement of u_L.

Lemma 3.1 Let $e = u - u_L$ and Pe be defined by (3.3) or (3.4). Assume η is sufficiently small (independently of ε). Then

$$||e - Pe||_{H^o_{p,\Delta}} \le C\,\eta\,||e||_{H^o_{p,\Delta}}, \quad 1 \le p \le \infty,$$

where C is independent of ε, Δ, and η.

Proof: By (2.3), (2.4) and Lemma 2.1 it follows that

$$||u||_{H^o_{p,\Delta}} = \sup_{v \in H^2_{q,\varepsilon,\Delta}} \frac{|B_\Delta(u,v)|}{||v||_{H^2_{q,\varepsilon,\Delta}}}, \qquad 1 \le p \le \infty.$$

Therefore,

$$(3.5) \qquad ||e - Pe||_{H^o_{p,\Delta}} = \sup_{v \in H^2_{q,\varepsilon,\Delta}} \frac{|B_\Delta(e-Pe,v)|}{||v||_{H^2_{q,\varepsilon,\Delta}}} .$$

For a given $v \in H^2_{q,\varepsilon,\Delta}$, let $w_v \in S_L^{(\eta)}$ be such that

$$(3.6) \qquad w_v(x) = \sum_{j=1}^{N} v(x_j)\psi^{(\eta)}_{-1,j}(x),$$

where $\psi^{(\eta)}_{-1,j}$ is defined by (2.8a). Clearly, $w_v(x_j) = v(x_j)$ and hence $v - w_v \in K_{B,q,\Delta}$. Therefore,

$$(3.7) \qquad B_\Delta(e-Pe, v-w_v) = 0.$$

Also, $w_v \in S_L^{(\eta)}$ implies that

$$(3.8) \qquad B_\Delta(e, w_v) = 0.$$

Equations (3.6) - (3.8) imply that

$$(3.9) \qquad |B_\Delta(e-Pe,v)| = |B_\Delta(Pe,w_v)|$$

$$= \Big| \sum_{j=1}^{N} \int_{I_j} (Pe)L^*(w_v) \Big| \le 2\eta ||v||_{L_\infty} ||Pe||_{L_p}.$$

Using (3.5) and (3.9) with Theorems 2.3 and 2.2 we obtain

$$||e-Pe||_{H^o_{p,\Delta}} \leq Cn||Pe||_{L_p}, \qquad 1 \leq p \leq \infty.$$

The desired result now follows provided n is sufficiently small.

As mentioned earlier $n = O(h)$, and hence if $E = ||Pe||_{L_p}$, then E is an asymptotically exact estimator to $||e||_{H^o_{p,\Delta}}$ by Lemma 3.1. However, we seek an estimator for $e_\alpha = u-u_\alpha$ where u_α is the finite element solution obtained by using $S_\alpha^{(k)}$ as the test space.

Let Pe_α denote the solution to the problem: find $Pe_\alpha \in K^1_{B,p,\Delta}$ such that

$$B_\Delta(Pe_\alpha,v) = B_\Delta(e_\alpha,v), \text{ for each } v \in K^2_{B,q,\Delta}, \quad 1 < q < \infty.$$

Pe_α also solves (3.3) with e replaced by e_α. Hence $Pe_\alpha \in H^o_{\infty,\Delta}$. By the triangle inequality we have

$$(3.10) \quad ||e_\alpha - Pe_\alpha||_{H^o_{p,\Delta}} \leq ||e_\alpha - e||_{H^o_{p,\Delta}} + ||e - Pe||_{H^o_{p,\Delta}}$$

$$+ ||Pe - Pe_\alpha||_{H^o_{p,\Delta}}.$$

First, consider the term $w = Pe - Pe_\alpha$. By (3.3), w solves the equation

$$Lw = L(u_\alpha - u_L)|_{I_j} \quad \text{in } I_j$$

$$w(x_{j-1}) = w(x_j) = 0, \quad j = 1,\ldots,N.$$

It follows from the maximum principle, specifically see [19] Lemma 4.1, that if h_j is sufficiently small, then

$$(3.11) \qquad ||w||_{L_\infty(I_j)} \le C \min\left(\frac{h_j}{a}, \frac{2h_j^2}{\varepsilon}\right) ||L(u_L - u_\alpha)||_{L_\infty(I_j)} .$$

On I_j,

$$L(u_L - u_\alpha) = -\varepsilon(u_L - u_\alpha)'' + a(x)(u_L - u_\alpha)' + b(x)(u_L - u_\alpha),$$

and hence by the local inverse theorem (since $u_L - u_\alpha \in S_r$), we have

$$(3.12) \qquad ||L(u_L - u_\alpha)||_{L_\infty(I_j)} \le C\left[\frac{\varepsilon}{h_j^2} + \frac{1}{h_j} + 1\right] ||u_L - u_\alpha||_{L_\infty(I_j)}.$$

Combining (3.11), (3.12), and Theorem 2.4d we obtain

$$(3.13) \qquad ||Pe_\alpha - Pe||_{L_\infty} \le C \max_j h_j^{r+2} ,$$

where C depends on a(x), b(x), and f(x), but is independent of ε, and h.

Beginning with (3.10), and applying Theorem 2.4, Lemma 3.1, and inequality (3.13), we obtain the following result.

Theorem 3.2. Let $e_\alpha = u - u_\alpha$, where u_α is the finite element solution obtained when using $S_\alpha^{(k)}$, with $k = 2r + 1$, as the test space. Let Pe_α be the projection of e_α into $K^1_{B,p,\Delta}$ defined by

$$B_\Delta(Pe_\alpha, v) = B_\Delta(e_\alpha, v) \quad \text{for each } v \in K^2_{B,q,\Delta},\ 1 < q < \infty.$$

Then by assumption A.3, $Pe_\alpha \in H^o_{\infty,\Delta}$, and

$$||e_\alpha - Pe_\alpha||_{H^o_{p,\Delta}} \le C_1 h ||e_\alpha||_{H^o_{p,\Delta}} + C_2 \max_j h_j^{r+2}, \quad \text{for } 1 \le p \le \infty.$$

If a lower bound on the error of the type

$$(3.14) \qquad ||e_\alpha||_{H^o_{p,\Delta}} \ge Ch^{r+1}$$

is available, where C can be chosen independently of ε and Δ, then it follows from Theorem 3.2 that

$$\left|1 - \frac{||Pe_\alpha||_{H^o_{p,\Delta}}}{||e_\alpha||_{H^o_{p,\Delta}}}\right| \leq \frac{||e_\alpha - Pe_\alpha||_{H^o_{p,\Delta}}}{||e_\alpha||_{H^o_{p,\Delta}}} \leq C_1\eta + C_2 h.$$

Since $\eta \leq Ch$, it follows that $E = ||Pe_\alpha||_{H^o_{p,\Delta}}$ is an asymptotically exact error estimator.

In order to justify (3.14), it suffices, for example, to suppose that there is an interval $I_o \subseteq I$ for which

$$u \in C^\infty(\bar{I}_o), \quad \text{but } u \notin S_r(I_o),$$

and there exists a constant $C > 0$ such that for all meshes Δ in some class

$$\min\{h_j : I_j \subseteq I_o\} \geq Ch(\Delta).$$

For further details see [12]. In practice these conditions are not very demanding, and no restrictions in the algorithm need be imposed.

We must now determine a way to compute $||Pe_\alpha||_{H^o_{p,\Delta}} = E$. This value E need not be computed exactly (in general this is not possible), but it could be approximated by some value E_A, provided that E_A is also an asymptotically exact estimator.

Let $w = Pe_\alpha$. Then w solves

$$-\varepsilon w'' + aw' + bw = \rho \quad \text{on } I_j$$

$$w(x_{j-1}) = w(x_j) = 0,$$

where $\rho = f - Lu_\alpha$ is the residue. If we rescale this problem to $I = [0,1]$,

using the notation $\tilde{g}(y) = g(x_{j-1} + h_j y)$ for $y \in [0,1]$, and dropping the index j, the function $\tilde{w}(y)$ solves

$$(3.15) \qquad L_h \tilde{w} \equiv -\frac{\varepsilon}{h^2}\tilde{w}'' + \frac{\tilde{a}}{h}\tilde{w}' + \tilde{b}\tilde{w} = \tilde{\rho} \quad \text{in } I,$$

$$\tilde{w}(0) = \tilde{w}(1) = 0.$$

Consider the case when r = 1, i.e., linear trial functions. Let $\tilde{w}_A$ be the solution to

$$(3.16) \qquad \hat{L}_h(\tilde{w}_A) \equiv -\frac{\varepsilon}{h^2}\tilde{w}_A'' + \frac{a_1}{h}\tilde{w}_A' = \tilde{\rho}_I \quad \text{in } I,$$

$$\tilde{w}_A(0) = \tilde{w}_A(1) = 0,$$

where $a_1 = \tilde{a}(1)$, and ρ_I is the linear interpolant of ρ. The function $\tilde{w}_A(y)$ is calculated explicitly in (3.31). Assume that $h_j^{1/p}||\tilde{w}_A||_{L_p(I)} = ||w_A||_{L_p(I_j)}$ $= \tau_j$ can also be calculated exactly. The value τ_j will be used as a local error indicator and the estimator E_A is calculated by

$$E_A = \left[\sum_{j=1}^{N} \tau_j^p\right]^{1/p}.$$

In order to prove that E_A is an asymptotically exact estimator the following results are needed.

Lemma 3.3 The Green's functions $G_h(x|y)$ and $\hat{G}_h(x|y)$ for the operators L_h and $\hat{L}_h$ are positive and satisfy the following inequalities:

$$(3.17) \qquad G_h(x|y) \le Ch(1-e^{-\tilde{\gamma}h/\varepsilon})/\tilde{\gamma}, \quad \text{for all } x,y \in [0,1],$$

$$(3.18)\quad \hat{G}_h(x|y) \le h(1-e^{-a_1 h/\varepsilon})/a_1, \quad \text{for all } x,y \in [0,1],$$

and

$$(3.19)\quad \hat{G}_h(x|y) \ge yh(1-e^{-a_1 h/4\varepsilon})/4a_1, \quad \text{for } 0 \le y \le x, \text{ and } \frac{1}{4} \le x \le \frac{3}{4},$$

where C is independent of ε and h, $\tilde{\gamma} = (a_1^2 + 4\varepsilon\underline{\tilde{b}})^{1/2}$, $a_1 = \tilde{a}(1)$, and $\underline{\tilde{b}} = \min \tilde{b}(y)$.

Proof: Inequalities (3.17) and (3.18) follow directly from rescaling the bound on the Green function established in [19], in proof of Theorem 2.5. For y in (0,x), $G_h(x|y)$ satisfies

$$\hat{L}_h^* \hat{G}_h(x|y) \equiv -\frac{\varepsilon}{h^2}(\hat{G}_h)_{yy} - \frac{a_1}{h}(\hat{G}_h)_y = 0 \quad ,$$

with boundary conditions

$$\hat{G}_h(x|0) = 0, \text{ and } \hat{G}_h(x|x) = g(x).$$

where

$$g(x) = \frac{h^2}{\varepsilon}\left[\int_0^x e^{ha_1(t-x)/\varepsilon}dt\right]\left[\int_x^1 e^{ha_1 t/\varepsilon}dt \Big/ \int_0^1 e^{ha_1 t/\varepsilon}dt\right].$$

For $x \in \left[\frac{1}{4}, \frac{3}{4}\right]$, $g(x) \ge \frac{h}{4a_1}\left[1 - e^{-ha_1/4\varepsilon}\right]$.

Let $z(y) = \frac{hy}{4a_1}[1 - e^{-ha_1/4\varepsilon}]$. Then

$$\hat{L}_h^* z(y) < 0$$

$$z(0) = 0, \quad \text{and}$$

$$z(x) \le g(x).$$

From the maximum principle it follows that $G_h(x|y) \geq z(y)$ if $\frac{1}{4} \leq x \leq \frac{3}{4}$, and $0 \leq y \leq x$.

Theorem 3.4 Let $\tilde{w}$ and $\tilde{w}_A$ be as defined in (3.15) and (3.16), respectively. Assume that the approximate solution u_α is piecewise linear, i.e., $r = 1$. Then

$$||\tilde{w} - \tilde{w}_A||_{L_p(I)} \leq C_1 h ||\tilde{w}_A||_{L_p(I)} + C_2 h^3.$$

Proof: Since our attention will always be focused on the rescaled functions on the interval $I = [0,1]$ the "tilda" notation is dropped for this proof. For a function $g(y)$ on I we use the notation $g_o = g(0^+)$ and $g_1 = g(1^-)$, and g_I is the linear interpolant of g, i.e. $g_I(y) = g_o + y(g_1 - g_o)$. To avoid confusion with $f_o(x)$ (see Assumption A3) we write $f(x) = f_o(x)$ in this proof.

Let $z = w - w_A$. Then z solves

$$L_h z \equiv \frac{\varepsilon}{h^2} z'' + \frac{\tilde{a} z'}{h} + \tilde{b} z = \rho - \rho_I - \frac{(a(y) - a_1)}{h} w_A' - b(y) w_A, \quad \text{in } I,$$

$$z(0) = z(1) = 0.$$

Write $z = z_A + z_B + z_C$ where

$$(3.20) \qquad L_h z_A = \rho - \rho_I, \qquad z_A(0) = z_A(1) = 0,$$

$$(3.21) \qquad L_h z_B = -\frac{(a - a_1)}{h} w_A', \quad z_B(0) = z_B(1) = 0,$$

and

$$(3.22) \qquad L_h z_C = -b w_A, \qquad z_C(0) = z_C(1) = 0.$$

First, Consider $z_A(y)$. By assumption A4, $a(x)$, $b(x)$, and $\delta(x)$ are piecewise smooth. Also $u_\alpha(x)$ is piecewise linear, and bounded (Theorem 2.4). Therefore,

$$(\rho-\rho_I)(y) = h^2[K_A(y) + u_\alpha' K_B(y)] \tag{3.23}$$

where $K_A(y)$ and $K_B(y)$ are bounded independently of ε and h. By (3.20) and (3.23)

$$z_A(x) = h^2 \int_0^1 \left[K_A(y) + u_\alpha' K_B(y)\right] G_h(x|y)dy. \tag{3.24}$$

Similarly, we may write

$$\rho_I(y) = \rho_o + y(\rho_1-\rho_o) = \rho_o + yh[\gamma_A + u_\alpha' \gamma_B] , \tag{3.25}$$

where γ_A and γ_B are independent of ε and h. From (3.16) and (3.25) we have

$$w_A(x) = \int_0^1 (\rho_o + hy\gamma_B u_\alpha')\hat{G}_h(x|y)dy + \int_0^1 hy\gamma_A \hat{G}_h(x|y)dy . \tag{3.26}$$

We now consider two separate cases.

Case 1. $|\delta_o - b_o u_\alpha(x_{j-1})| \geq \frac{1}{2}|a_o u_\alpha'|$. In this case u_α' is bounded, and hence, from (3.24) and Lemma 3.3,

$$|z_A(x)| \leq Ch^3 . \tag{3.27}$$

Case 2. $|\delta_o - b_o u_\alpha(x_{j-1})| < \frac{1}{2}|a_o u_\alpha'|$. In this case

$$\rho_o = |\delta_o - b_o u_\alpha(x_{j-1}) - a_o u_\alpha'| \geq \tfrac{1}{2}|a_o u_\alpha'| .$$

This is further broken down into two subcases where either $|u_\alpha'| \leq 1$ or $|u_\alpha'| > 1$. If $|u_\alpha'| \leq 1$ we have (3.27) again. If $|u_\alpha'| > 1$, (3.26), (3.19), (3.23) and (3.17) imply that for h sufficiently small,

$$||w_A||_{L_p} \leq C\,(1-e^{-a_1 h/4\varepsilon})|u'_\alpha|h$$

and

$$||z_A||_{L_p} \leq C\,(1-e^{-\gamma h/\varepsilon})|u'_\alpha|h^3 \quad . \tag{3.28}$$

Thus,

$$||z_A||_{L_p} \leq Ch^2||w_A||_{L_p} \quad .$$

When considering the term z_B, since a is smooth,

$$\frac{a_1 - a(y)}{h}\, w'_A = C_a(y)(1-y)w'_A$$

where $C_a(y)$ is bounded independently of ε and h. Let $t = 1 - y$ and define v(t) by

$$v(t) = tw'_A(1-t) + w_A(1-t) \quad .$$

Then $v(0) = 0$ and v solves

$$-\frac{\varepsilon}{h^2}\, v'(t) - \frac{a_1}{h}\, v(t) = q(t) \quad ,$$

where $q(t) = -t\rho_I(1-t) - \frac{a_1}{h}\, w_A(1-t)$.

Therefore,

$$||v||_{L_1} \leq \frac{h}{a_1}\,(1-e^{-a_1 h/\varepsilon})||q||_{L_1} \quad \text{and}$$

$$||\frac{(a_1-a(y))}{h}\, w'_A||_{L_1} \leq \frac{Ch}{a_1}(1-e^{-a_1 h/\varepsilon})||\rho_I||_{L_1} + C\,||w_A||_{L_1} \quad .$$

From this, (3.21) and (3.18),

$$|z_B(x)| \leq Ch^2(1-e^{-a_1 h/\varepsilon})||\rho_I||_{L_1} + Ch||w_A||_{L_1} .$$

We must now show that either $||\rho_I||_{L_1} \leq C h^{-1}||w_A||_{L_1}/(1-e^{-a_1 h/\varepsilon})$ or $||\rho_I||_{L_1} \leq C h$. This can be shown by arguments analogous to those used discussing $||z_A||_{L_p}$. The same two cases are distinguished as before. In addition Case 1 is split into two subcases: $|\rho_o| \geq 2|\rho_1-\rho_o|$ and $|\rho_o| < 2|\rho_1-\rho_o|$.

Therefore,

$$||z_B||_{L_p} \leq C_1 h||w_A||_{L_1} + C_2 h^3 . \tag{3.29}$$

From (3.22) and (3.18) we have

$$||z_C||_{L_p} \leq Ch||w_A||_{L_1} . \tag{3.30}$$

The theorem follows from the fact that $w-w_A = z_A + z_B + z_C$ and inequalities (3.27)-(3.30).

Corollary 3.5. Suppose that (3.14) holds. Let

$$E_A = \begin{cases} \left[\sum \tau_j^p\right]^{1/p} & 1 \leq p \leq \infty, \\ \max\limits_j \tau_j & p = \infty, \end{cases}$$

where $\tau_j = h_j^{1/p}||\tilde{w}_A||_{L_p(I)}$ with $\tilde{w}_A$ defined in (3.16). Then E_A is an asymptotically exact estimator to $||e_\alpha||_{H^o_{p,\Delta}}$ for $1 \leq p \leq \infty$, when $r = 1$.

Proof: This result follows from the triangle inequality and Theorems 3.2 and 3.4. Finally, we remark that Corollary 3.5 also holds when the effects of quadrature are included. For details, again see [18].

The problem of explicitly calculating $||w_A||_{L_p(I)}$ still remains. From (3.16) we have

$$\tilde{w}_A(y) = A + Be^{h_j a_1 y/\epsilon} + Cy^2 + Dy \tag{3.31}$$

where

$$C = h_j(R_1 - R_o)/2a_1$$

$$D = h_j R_o/a_1 + (R_1 - R_o)/a_1^2$$

$$A = -(C + D)/(1-e^{h_j a_1/\epsilon})a_1^2$$

$$B = -A$$

As before, $a_1 = \tilde{a}(1) = a(x_j)$, $R_o = \tilde{R}(0) = R(x_{j-1}^+) = \delta(x_{j-1}^+) - a_o u_h'|_{I_j} - b_o u_h(x_{j-1})$ and $R_1 = \tilde{R}(1) = R(x_j^-)$.

When $p = 2M$, where M is a positive integer, $\tau_j = h_j||w_A||_{L_p(I)}$ can be computed exactly. However, all of the numerical results presented in the next chapter are performed with $p = 1$. We do not know a-priori if $\tilde{w}_A$ will change sign or not, and if it does, the zero of $\tilde{w}_A$ cannot be determined explicitly. Therefore, if $\tilde{w}_A$ changes sign in I we cannot compute $||w_A||_{L_1}$ exactly.

Suppose that we let

$$\tau_j^* = h_j\left|\int_0^1 \tilde{w}_A dy\right|$$

which can be easily calculated from (3.31). The next theorem shows that with certain assumptions on the exact solution u, if

$$E_A^* = \sum_{j=1}^{N} \tau_j^*$$

then E_A^* is an asymptotically exact estimator to $||\epsilon_\delta||_{H^o_{1,\Delta}}$.

Theorem 3.6. Let u be the exact solution and suppose that u'' does not change sign on any interval I_j, $j = 1,\ldots,N$. Also assume that u is such that (3.14) holds for r = 1. Then, if $\tau_j^* = h_j\left|\int_0^1 \tilde{w}_A\right|$ and $E_A^* = \sum_{j=1}^{N} \tau_j$, then E_A^* is an asymptotically exact estimator to $||e_\alpha||_{H^o_{1,\Delta}}$, where $e_\alpha = u - u_\alpha$.

Proof. By the triangle inequality, and Theorems 3.2 and 3.4 it follows that

$$(3.32)\quad ||e_\alpha - w_A||_{H^o_{1,\Delta}} \le ||e_\alpha - Pe_\alpha||_{H^o_{1,\Delta}} + ||Pe_\alpha - w_A||_{H^o_{1,\Delta}}$$

$$\le C_1 h||e_\alpha||_{H^o_{1,\Delta}} + C_2 h^3.$$

Also, since $w_A(x_j) = 0$, $j = 0,\ldots,N$

$$(3.33)\quad ||e_\alpha - w_A||_{H^o_{1,\Delta}} = ||e_\alpha - w_A||_{L_1(I)} + \sum_{j=1}^{N} |e_\alpha(x_j)|\rho_j.$$

Inequality (3.32), and (3.33) imply that

$$(3.34)\quad \sum_{j=1}^{N} |e_\alpha(x_j)|\rho_j \le C_1 h||e_\alpha||_{H^o_{1,\Delta}} + C_2 h^3.$$

Let $e_\alpha^* = e_\alpha - e_{\alpha I}$, where $e_{\alpha I}$ is the linear interpolant of e_α. Then,

$$(3.35)\quad ||e_\alpha - e_\alpha^*||_{H^o_{1,\Delta}} = ||e_{\alpha I}||_{H^o_{1,\Delta}} \le 2 \sum_{j=1}^{N} |e_\alpha(x_j)|\rho_j$$

$$\le C_1 h||e_\alpha||_{H^o_{1,\Delta}} + C_2 h^3.$$

This shows that $||e_\alpha^*||_{L_1}$ is an asymptotically exact estimator for $||e_\alpha||_{H^o_{1,\Delta}}$.

Since e^*_α does not change concavity on I_j, and $e^*_\alpha(x_{j-1}) = e^*_\alpha(x_j) = 0$,

$$||e^*_\alpha||_{L_1(I_j)} = \left| \int_{I_j} e^*_\alpha \right|.$$

So

$$\begin{aligned} |||e^*_\alpha||_{L_1(I)} - E^*_A| &= \left| \sum_{j=1}^{N} ||e^*_\alpha||_{L_1(I_j)} - \sum_{j=1}^{N} \left| \int_{I_j} w_A dy \right| \right| \\ &= \left| \sum_{j=1}^{N} \left| \int_{I_j} e^*_\alpha \right| - \left| \int_{I_j} w_A \right| \right| \\ &\leq \sum_{j=1}^{N} \left| \int_{I_j} e^*_\alpha - w_A \right| \\ &\leq ||e^*_\alpha - w_A||_{L_1(I)} \leq ||e_\alpha - w_A||_{L_1} + ||e_{\alpha I}||_{L_1} \\ &\leq C_1 h ||e_\alpha||_{H^o_{1,\Delta}} + C_2 h^3, \end{aligned}$$

where the last inequality followed from (3.32) and (3.35).

The assumption u" doesn't change sign locally, if violated, will in general not disrupt the effectivity of the error estimator E*. If u" does change sign in some interval I_j, then I_j cannot lie within the boundary layer or interior layer of the solution u. This is because in the boundary layer region, $|u''| \geq C\varepsilon^{-1}$, where C is independent of ε (see e.g. [10]). Suppose that u is smooth in this interval and that u" is bounded in I_j independently of ε. Then, since u" vanishes at some point in I_j,

$$|e^*_\alpha(x)| = |u(x) - u_I(x)| \leq Ch_j^2 |u''(\xi_x)| \leq Ch_j^3, \quad \text{for } x \in I_j.$$

The value $||e_\alpha^*||_{H_{1,\Delta}^o}$ is an asymtotically exact estimator by Theorem 3.6, and also, by assumption (3.14),

$$\sum_{j=1}^{N} ||e_\alpha^*||_{L_1} \geq Ch^2.$$

Since $||e_\alpha^*||_{L_1(I_j)} \leq Ch_j^4$, the error on this interval is one higher order than can be expected by the best approximation to u by a linear function on I_j. Thus, in general, the error in this interval is negligible in its contribution to the total error or an asymptotically exact error estimate. Even with this consideration, the following precautionary measure is taken just in case this assumption is violated.

Let

$$Q(\xi) = h_j \left| \int_o^\xi \tilde{w}_A(t)dt - \int_\xi^1 \tilde{w}_A(t)dt \right| .$$

By (3.31) $\tilde{w}_A$ can have at most one zero in the open interval (0,1). If $\tilde{w}_A(\xi) = 0$ and $\xi \in (0,1)$, then $Q(\xi) = h_j||\tilde{w}_A||_{L_1} = \tau_j$. Also note that $Q(1) = \tau_j^*$. Let $h_j||\tilde{w}_A||_Q = \max_{i=1,\ldots,4} Q(\xi_i)$, where

$$\xi_1 = 1/3, \qquad \xi_2 = 1/2$$

$$\xi_3 = 2/3, \quad \text{and} \qquad \xi_4 = 1.$$

Then $||\cdot||_Q$ is a norm over the space of functions $\tilde{w}_A$ defined in (3.31). Since this space is only two dimensional the norms $||\cdot||_Q$ and $||\cdot||_{L_1}$ are equivalent on this space. Therefore, if $\tau_j' = h_j||\tilde{w}_A||_Q$, then $C_1 \leq \frac{\tau_j'}{\tau_j} \leq C_2$, and furthermore the constants C_1 and C_2 are independent of ε

and h. Thus, even if the assumption on u" is violated, we can still quarantee that the estimator $E'_A = \tau'_j$ satisfies

$$C_1 \leq \frac{E'_A}{||e_\alpha||_{H^o_{1,\Delta}}} \leq C_2 ,$$

with C_1 and C_2 independent of ε, and Δ. For the computations presented in the following chapter, $\tau'_j = h_j ||\tilde{w}_A||_Q$ was used as the error indicator for I_j.

In conclusion of this chapter we state a superconvergence result for the errors at the nodal points.

Corollary 3.7: (Nodal superconvergence)

The nodal errors $e_\alpha(x_j)$ satisfy

$$\left[\sum_{j=1}^{N} |e_\alpha(x_j)|^p \rho_j \right]^{1/p} \leq C_1 h ||e_\alpha||_{H^o_{p,\Delta}} + C_2 h^3. \quad 1 \leq p \leq \infty.$$

Proof: For p = 1 this is (3.34). For p > 1, the result follows by appropriately modifying (3.32) and (3.33).

CHAPTER 4

NUMERICAL RESULTS

As mentioned in the introduction, the equilibriation of the error indicators τ_j leads to an optimal mesh. An effective algorithm for performing this task has been developed by Babuska and Rheinboldt, and implemented in FEARS (Finite Element Adaptive Research Solver) ([2], [4], [11], [15]). This algorithm makes a prediction on the error indicators after a future subdivision. The predictions are calculated by assuming that the indicator of an element will decrease by essentially the same ratio as the last time it was subdivided. The maximum predicted error is then used as the threshold value for subdivision--all elements with indicators above the threshold are refined. The algorithm continues to solve and then refine until the desired accuracy is attained.

Example 1 is a typical linear convection diffusion equation in which all assumptions A1-A4 hold. A detailed description of the effectivity index θ and the rates of convergence for both uniform and adaptive meshes is presented. Example 2 is a linear problem with a turning point which violates assumption A1. Nevertheless, this problem was succesfully solved by the algorithm. Example 3 is a non-linear turning point problem. The robustness of the method is best displayed through the results obtained for this problem. In all examples linear elements were used for the trial space.

Example 1: Consider the problem:

$$(4.1) \quad -\varepsilon u'' + u' + (1+\varepsilon)u = -\beta - \varepsilon\alpha + (1+\varepsilon)(\alpha-\beta)x \text{ in } (0,1)$$

$$u(0) = u(1) = 0$$

where $\alpha = 1 + e^{-(1+\varepsilon)/\varepsilon}$ and $\beta = 1 + e^{-1}$. The exact solution to this problem is

$$u(x) = e^{(1+\varepsilon)(x-1)/\varepsilon} + e^{-x} - \alpha + (\alpha - \beta)x.$$

This problem was studied by Kellogg and Han [9] , with the use of enriched spaces. We remark that the results presented for this problem were typical for all linear problems satisfying A1-A4.

The adaptive process of computing the error indicators, refining, and then resolving, was initiated on a uniform mesh of four elements. The results of each solution pass of the iteration for $\varepsilon = .01$ are summarized in Table 1.

TABLE 1

Summary of results for the adaptive mesh refinement procedure used on (4.1) with $\varepsilon = .01$.

NUMBER OF ELEMENTS	MAXIMUM NODAL ERROR	RELATIVE ERROR IN $H^o_{1,\Delta}$	EFFECTIVITY θ
4	2.70E-4	1.19E-1	1.0877
5	2.62E-4	5.15E-2	1.0442
6	2.62E-4	2.27E-2	1.0204
7	2.62E-4	9.53E-3	1.0085
8	2.62E-4	4.99E-3	1.0067
12	2.97E-5	1.72E-3	1.0052
23	3.91E-6	4.68E-4	1.0034
35	2.05E-6	2.11E-4	1.0043
55	2.56E-7	7.65E-5	1.0009
102	1.77E-8	2.21E-5	1.0005
201	1.18E-9	5.69E-6	1.0003

One of the most important aspects of these computations is the effectivity index θ of the error estimate. Recall $\theta = E/||e||_{H^o_{1,\Delta}}$, where

$\tilde{E}$ is the computed error estimate and $e = u - u_h$ is the exact error. The values as listed in Table 1 reveal that the error estimate at worst is within 8.8% of the true error, and this percentage decreases rapidly as the mesh is refined.

Graphs of the effectivity index are presented in Figures 1 and 2 as a function of the number of elements. Figure 1 displays the values of θ using uniform meshes for ε in the range 10^{-10} to 1. Again, notice the improvement in θ as the number of elements increases. The rate of decrease of $|1-\theta|$ on uniform meshes is $O(N^{-1})$ for $\varepsilon \leq 10^{-4}$, and $O(N^{-2})$ for $\varepsilon \geq 10^{-1}$. Furthermore, the fact that the graphs of $\theta = \theta_\Delta(\varepsilon,N)$ are nearly superimposed for $\varepsilon \leq 10^{-3}$ indicates that $\theta_\Delta(\varepsilon,N)$ converges as $\varepsilon \to 0$. The values $\theta_\Delta(0^+,N)$ provide an upper bound for $\theta_\Delta(\varepsilon,N)$ on uniform meshes Δ.

Figure 2 compares the effectivities when $\varepsilon = 10^{-6}$ using both uniform and adaptively constructed meshes. With adaptive meshes, the graph of $\theta_\Delta(\varepsilon,N)$ is no longer smooth, but it still lies beneath the graph of θ for uniform meshes. This behavior was typical for all values of ε tested. The improvement of the effectivities using adaptive meshes was even more profound on other problems (see Example 2 or [18]).

Next, we examine the rates of convergence attained in the $H^o_{1,\Delta}$ norm. If $N = N(\Delta)$ is the number of degrees of freedom in the mesh, we will assume that the error $E_N = ||e||_{H^o_{1,\Delta}}$ has the form $E_N = CN^{-\gamma}$. The rate γ is assumed to depend on both ε and R, i.e., $\gamma = \gamma(\varepsilon,R)$, where R is the relative error $\dfrac{E_N}{||u||_{H^o_{1,\Delta}}}$. Figure 3 shows the graphs of $\gamma(\varepsilon,.1)$, $\gamma(\varepsilon,.01)$ and $\gamma(\varepsilon,.0025)$, when uniform meshes are used. For $R \leq .01$ the graphs begin with a value of two and then decrease to one (or nearly one), as $\varepsilon \to 0$. This transition from two to one is delayed, as smaller relative errors are considered. The optimal

rates of convergence (N^{-2} if $1/N < \varepsilon$, and N^{-1} if $1/N >> \varepsilon$) for uniform meshes are reflected by these graphs.

Figure 4 shows the graphs of $\gamma(\varepsilon, 10^{-2})$, $\gamma(\varepsilon, 10^{-3})$, and $\gamma(\varepsilon, 10^{-5})$, when adaptively constructed meshes are employed. Notice that these graphs always lie above or on the value $\gamma = 2$, which implies that the rates of convergence observed are always $O(N^{-2})$. It is also important to note that when using adaptive meshes, the rate of convergence is unharmed as $\varepsilon \to 0$.

The rates of convergence using adaptive and uniform meshes for $\varepsilon = 1$, .01. and .0001, can also be seen from the slopes of the graphs of the relative $H^o_{1,\Delta}$ errors, displayed in Figure 5. By extrapolating the graph of the error for $\varepsilon = .0001$ using uniform meshes, it can be seen that in order to obtain the same accuracy achieved with an adaptive mesh of 149 elements, approximately 17,000 uniform elements would be required. For smaller values of ε this effect is even more pronounced.

The maximum nodal errors for this problem are displayed in Figure 6. In each case, using both uniform and adaptively constructed meshes for $\varepsilon = 1.0$, and .0001, the superconvergent rate of $O(N^{-3})$ is attained. Notice that when $\varepsilon = .0001$, the maximum nodal errors are smaller for uniform meshes than for adaptive meshes. This unexpected result does not contradict the theory — the adaptivity optimizes the mesh based on the errors in $H^o_{1,\Delta}$, without regard to the nodal errors.

To describe the distribution of the mesh points, we use the mesh grading function $\xi_\Delta(x)$. The function $\xi_\Delta(x)$ is the piecewise linear function on the mesh with the property

$$\xi_\Delta(x_j) = \frac{j}{N}, \qquad j = 0, \ldots, N.$$

For example, on a uniform mesh, $\xi_\Delta(x) = x$. The derivative of $\xi_\Delta(x)$ is a measure

of the density of the mesh points. The mesh points will be heavily concentrated in regions where $\xi_\Delta(x)$ increases rapidly.

Figure 7 shows the graph of the mesh grading function when $\varepsilon = .01$, for an adaptively constructed mesh of 201 elements. Note the heavy refinement in the boundary layer region (near $x = 1$). The remainder of the nodal points were distributed nearly uniformly throughout the rest of the interval. This reflects the fact that u is smooth (although not linear) outside of the boundary layer.

Example 2. Consider the following turning point problem:

$$(4.2)\quad -\varepsilon u'' - xu' = \varepsilon\pi^2\cos(\pi x) - (\pi x)\sin(\pi x) \text{ on } (-1,1),$$

$$u(-1) = -2, \qquad u(1) = 0.$$

The solution to this problem is

$$u(x) = \cos(\pi x) + \operatorname{erf}(x/\sqrt{2\varepsilon})/\operatorname{erf}(1/\sqrt{2\varepsilon}),$$

which has an interior layer at $x = 0$.

Although this equation violates assumption A1 at $x = 0$, the results presented here reveal the robustness of the algorithm and suggest that the crucial theoretical results also hold for this type of problem.

Figure 8 displays the graphs of the errors in the $H^o_{1,\Delta}$ norm for $\varepsilon = .01$ and .0001, using both uniform and adaptive meshes. The optimal rate of convergence ($O(N^{-2})$), is quickly realized in all cases. The errors using adaptive meshes are smaller than with uniform meshes, particularly when $\varepsilon = .0001$.

The graphs of the maximum nodal errors for $\varepsilon = .0001$ are presented in Figure 9. These graphs indicate that nodal superconvergence occurs even in the presence of a turning point, provided adaptive meshes are used.

Figure 10 displays the graphs of the effectivity indices, $\theta_\Delta(\varepsilon,N)$, for $\varepsilon = .01$, and .0001 using both uniform and adaptive meshes. Even on this turning point problem, we have good effectivity indices—at worst $\theta = 1.72$.

Example 3: Consider one-dimensional flow in a duct of variable cross sectional area. A one equation model for steady non-heat conducting, viscous flow has been developed by Shubin and Stephens in [16] and [17]. This model is governed by the equation

$$-\varepsilon u_{xx} + r_x + G = 0 \text{ on } (0,L) \tag{4.3}$$

where

$$G = -(\gamma-1)C\left(\frac{H}{u} - \frac{u}{2}\right) A'/A^2 +$$

$$+ \gamma(\tilde{D}u + E/u)A'/A^2,$$

$$r = \frac{\gamma}{A}(\tilde{D}u + E/u),$$

$\tilde{D} = D - \varepsilon A'$, $D = (\gamma+1)C/2\gamma$, and

$E = (\gamma-1)CH/\gamma$.

$\gamma = 1.4$ is the ratio of specific heats,

$C = .68471$ and $H = 3.5$ are constants,

$A(x) = 1.398 + .347 \tanh(.8x - 4)$ is the cross sectional area,

ε is the viscosity coefficient assumed to be constant, and

$u(x)$ is the velocity.

In the inviscid case ($\varepsilon = 0$), the velocity is sonic if $u = a = (E/D)^{\frac{1}{2}} = 1.0801$, supersonic if $u>a$ and subsonic if $u<a$. When the viscous problem is solved with boundary conditions such that $u(0)>a$ and $u(L)<a$ an interior layer arises. In the limiting case as $\varepsilon \to 0$, this layer becomes a shock. The boundary conditions used are $u(0) = 1.299$ and $u(L) = .505$ with $L = 10$.

We solve the nonlinear problem by iterating on a linearization of the equation. This procedure is described in [8] and referred to as a variant of Newton-Kantorovich method. In general, consider the nonlinear problem

$$-\varepsilon u'' + F(x,u,u') = 0 \text{ in } I = [x_o, x_N]$$

$$u(x_o) = \alpha, \quad u(x_N) = \beta$$

The linearized boundary value problem for the Newton-Kantorovich iteration is

$$(4.4) \qquad -\varepsilon u''_{m+1} + F_{u'}(x,u_m,u'_m)u'_{m+1} + F_u(x,u_m,u'_m)u_{m+1}$$
$$= F_u(x,u_m,u'_m)u_m + F_{u'}(x,u_m,u'_m)u'_m - F(x,u_m,u'_m) \text{ in } I,$$

$$u_{m+1}(x_o) = \alpha ,$$

$$u_{m+1}(x_N) = \beta ,$$

The aim was now to use the continuation method with respect to decreasing values of ε together with intermittent mesh refinements based on the linearized equation (4.4). This procedure was started using a large value of ε, a uniform mesh, and a linear solution u_o which satisfied the boundary conditions. For sufficiently large ε ($\varepsilon = .1$), the iterative process converged quickly. Using the continuation method, the value of ε would be decreased by a factor of about two. This would lead to convergence provided the mesh was sufficiently refined and the approximation was sufficiently close to the exact solution for the current ε. In this manner the adaptive method not only found accurate solutions and error estimates, but also significantly increased the efficiency of the continuations used.

The computed solutions for $\varepsilon = .1$, $.01$, and $.001$ are graphed in Figure 11. The exact inviscid solution, which has a shock at $x = 4.816$ is practically indistinguishable from the computed viscous solution with $\varepsilon = .001$. The effectivity indices and relative errors were also calculated with respect to the exact viscous solutions and are shown in Table 2.

TABLE 2

The effectivity indices and relative errors for the duct flow problem

ε	EFFECTIVITY INDEX	RELATIVE ERROR
.1	.78	.10E-2
.01	.83	.20E-3
.001	.77	.33E-4

The exact solutions were approximated by a computed solution on a sufficiently fine mesh. The mesh grading function for the ε = .001 solution with 84 elements is displayed in Figure 12.

The interior layer of the solution contains a turning point of the linearized equation (4.4). The turning point x_t occurs when $u_m(x_t) = (E/\tilde{D}(x_t))^{\frac{1}{2}}$ in which case $F_u,(x_t,u_m(x_t),u_m'(x_t)) = 0$. If this point occured in an interior region of an element, no upwinding was performed there. If F_u, was nearly zero at one endpoint of an element and sufficiently large at the other endpoint, then upwinding was performed based on the larger value. This corresponds to the "switching schemes" derived in [16] and [17].

REFERENCES

1. I. Babuška, The Adaptive Methods and Error Estimation for Elliptic Problems of Structural Mechanics, Proceedings of the ARO Workshop on Adaptive Methods for Partial Differential Equations, Univ. of Maryland, 14-16 February, 1983.

2. I. Babuška, W. Rheinboldt, Error Estimates for Adaptive Finite Element Computations, SIAM J. Numer. Anal. 15, (1978), pp. 736-754.

3. _____, Analysis of Optimal Finite Meshes in R^1, Math. Comput., 33 (1979), pp. 435-463.

4. _____, Reliable Error Estimation and Mesh Adaptation for the Finite Element Method, Computational Methods in Nonlinear Mechanics, J. T. Oden, ed., North-Holland Pub. Co., 1980, pp. 67-108.

5. _____, Computational Error Estimates and Adaptive Processes for Some Nonlinear Structural Problems, Comp. Meth. Appl. Mech. and Engng., 34 (1982), pp. 895-937.

6. J. W., Barrett, K. W. Morton, Optimal Finite Element Solutions to Diffusion Convection Problems in One Dimension, Int. J. Num. Meth. Engng., 15 (1980), pp. 1457-1474.

7. _____, Optimal Petrov-Galerkin Methods Through Approximate Symmetrization, IMA Journal of Num. Anal., 1 (1981), pp. 439-468.

8. P. W. Hemker, A Numerical Study of Stiff Two-Point Boundary Problems, Mathematisch Centrum, Amsterdam, 1977.

9. R. B. Kellogg, H. Han, The Finite Element Method for a Singular Perturbation Problem Using Enriched Subspaces, Univ. of Maryland, Instit. for Phys. Sci. and Tech., Technical Note BN-978, 1981.

10. R.B. Kellogg, A. Tsan, Analysis of Some Difference Approximations for a Singular Perturbation Problem Without Turning Points, Math. of Comp., 32, 1978 pp. 1025-1039.

11. C. Mesztenyi, W. Szymczak, FEARS User's Manual for UNIVAC 1100, Univ. of Maryland, Instit. for Phys. Sci. and Tech., Technical Note BN-991, 1982.

12. A. Miller, On Some A Posteriori Error Estimates in the Finite Element Method, Dissertation, Univ. of Queensland, 1981.

13. H.-J. Reinhardt, A-Posteriori Error Analysis and Adaptive Finite Element Methods for Singularly Perturbed Convection-Diffusion Equations, to appear in Math. Methods Appl. Sci.

14. _____, A-Posteriori Error Estimation for Finite Element Modifications of Line Methods Applied to Singularly Perturbed Partial Differential Equations, Christian-Albrechts-Universitat, Institut fur Informatik und Praktische Mathematik, Bericht Nr. 8207, 1982.

15. W. C. Rheinboldt, C. K. Mesztenyi, On a Data Structure for Adaptive Finite Element Mesh Refinements, ACM Trans. on Mathematical Software, 6.2 (1980), pp. 166-187.

16. G. R. Shubin, A. B. Stephens, Exponentially Derived Switching Schemes, in Computational and Asymptotic Methods for Boundary and Interior Layers, Proceedings of the BAIL II Conference, J. J. H. Miller, ed., Boole Press, Dublin, 1982, pp. 382-387.

17. A. B. Stephens, G. R. Shubin, Exponentially Derived Switching Schemes for Inviscid Flow, to appear.

18. W. G. Szymczak, An Adaptive Finite Element Method for Convection Diffusion Problems, Dissertation, Univ. of Maryland, 1982.

19. W. G. Szymczak, I. Babuška, An Analysis of a Finite Element Method for Convection-Diffusion Problems. Part I Quasioptimality, to appear.

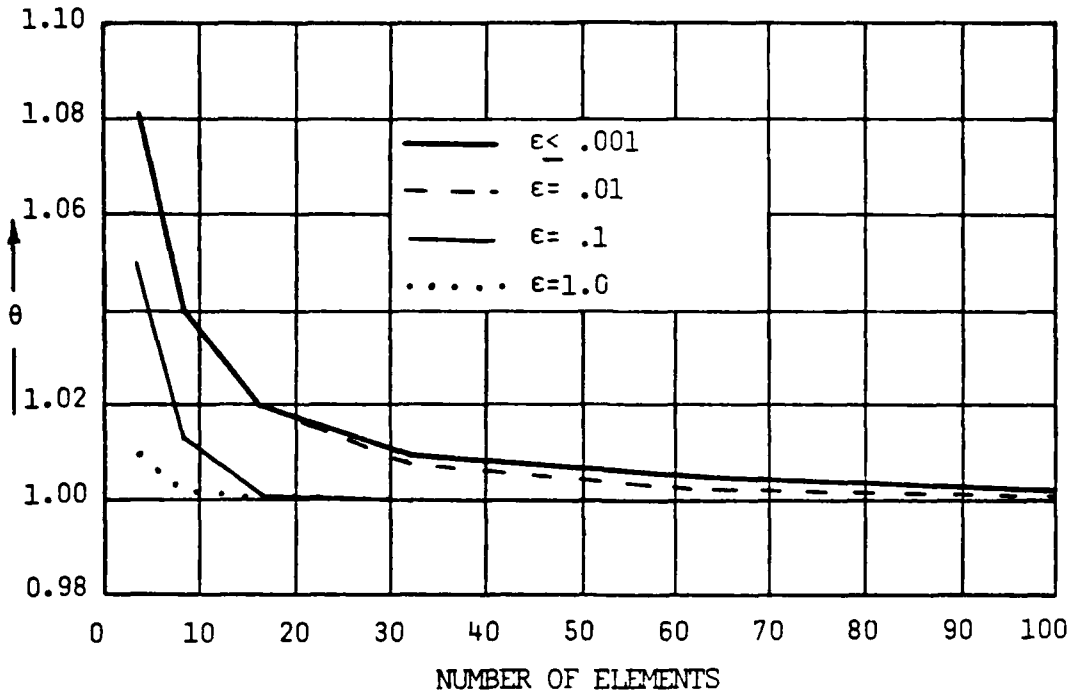

FIGURE 1: Effectivity indices for problem (4.1) with various values of ε using uniform meshes. For $\varepsilon \leq .001$, the values actually tested were $\varepsilon = 10^{-3}, 10^{-4}, 10^{-5}, 10^{-6}, 10^{-8}$, and 10^{-10}.

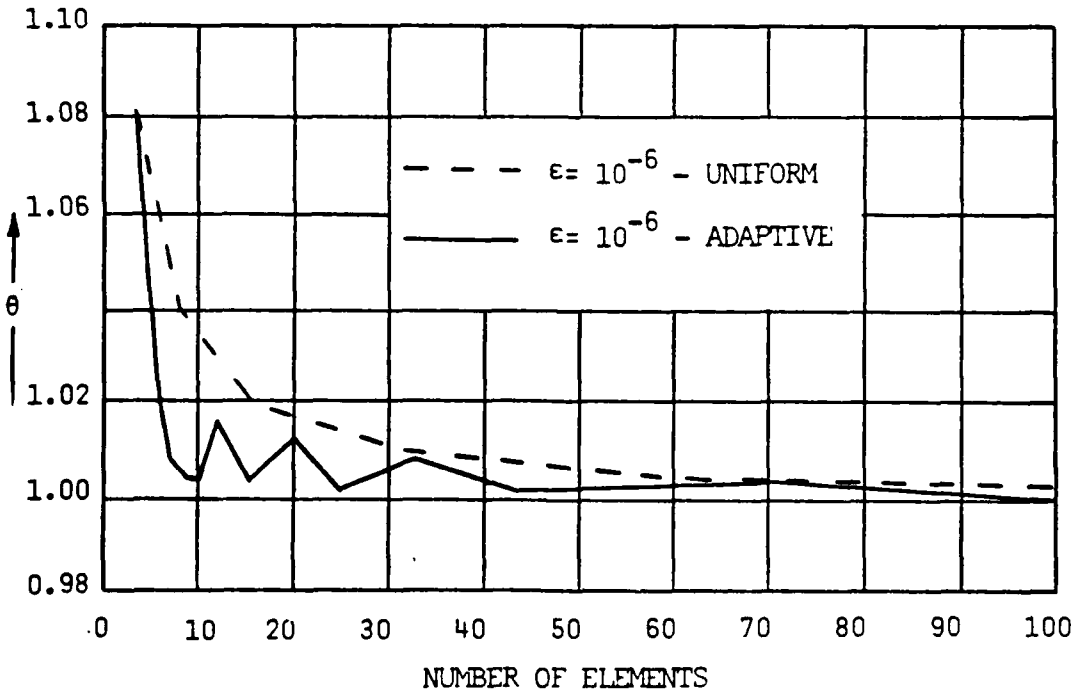

FIGURE 2: Effectivity indices for problem (4.1) when $\varepsilon=10^{-6}$ using adaptive and uniform meshes.

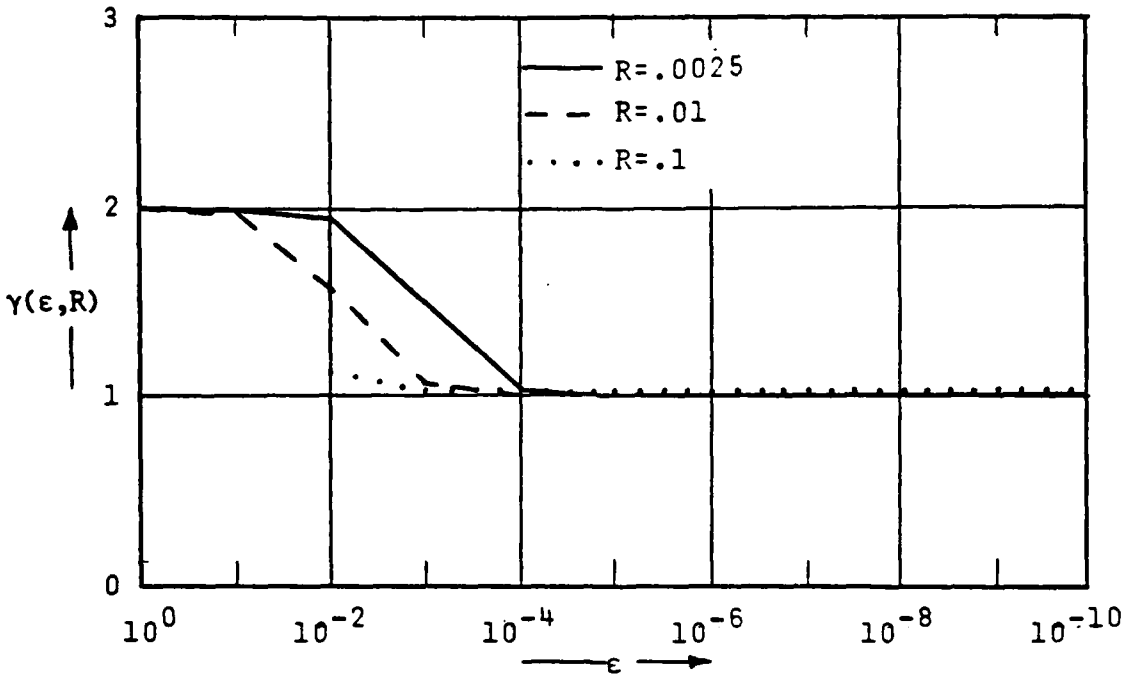

FIGURE 3: Rates of convergence for problem (4.1) at various relative errors using uniform meshes.

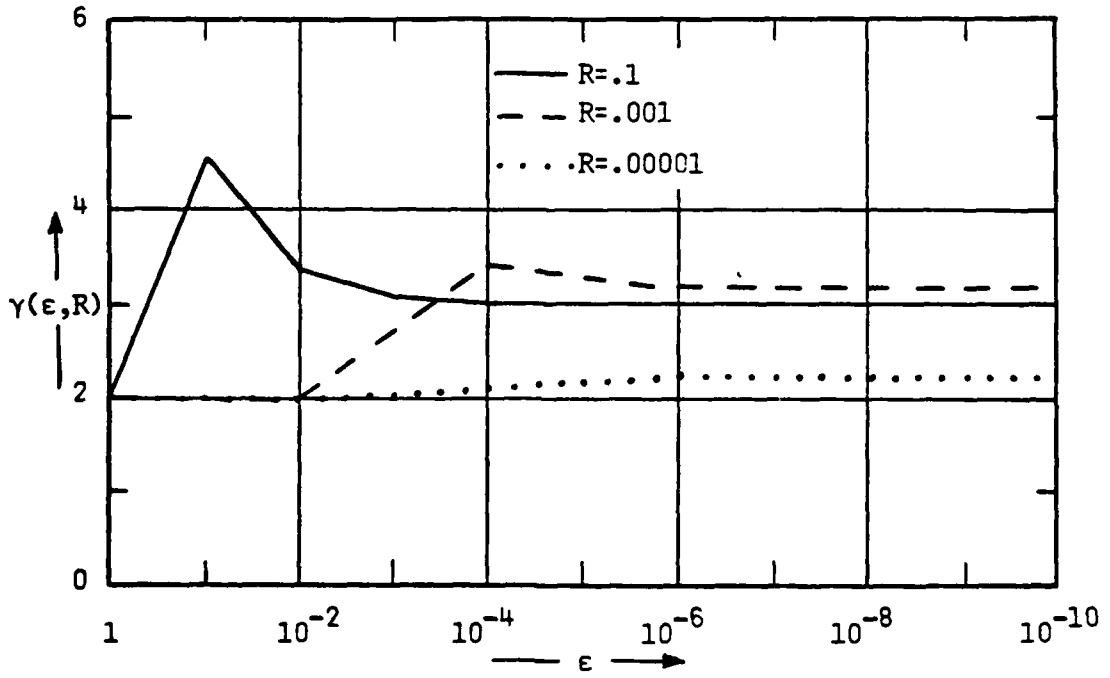

FIGURE 4: Rates of convergence for problem (4.1) at various relative errors using adaptive meshes.

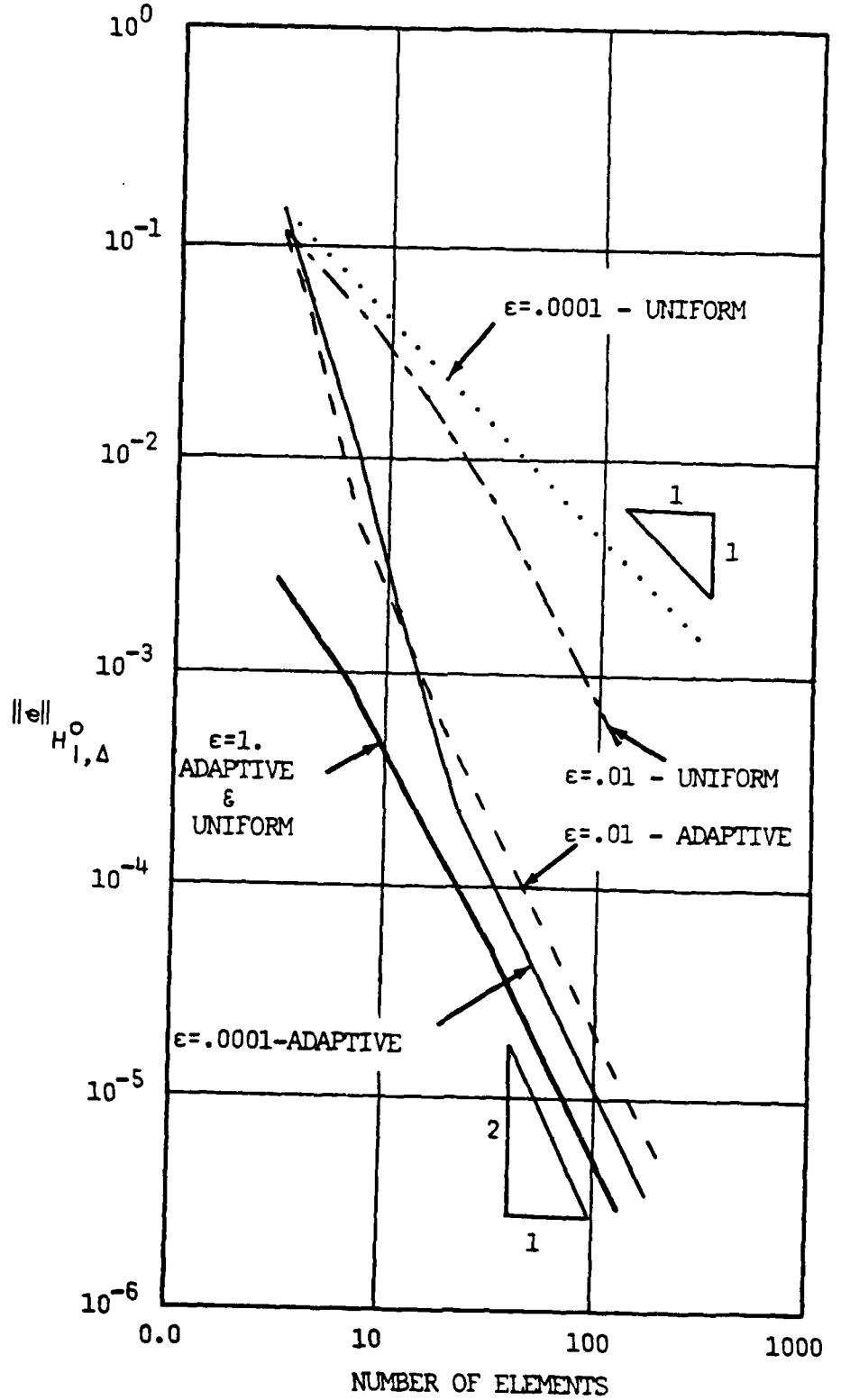

FIGURE 5: Errors in the $H^0_{1,\Delta}$ norm for problem (4.1).

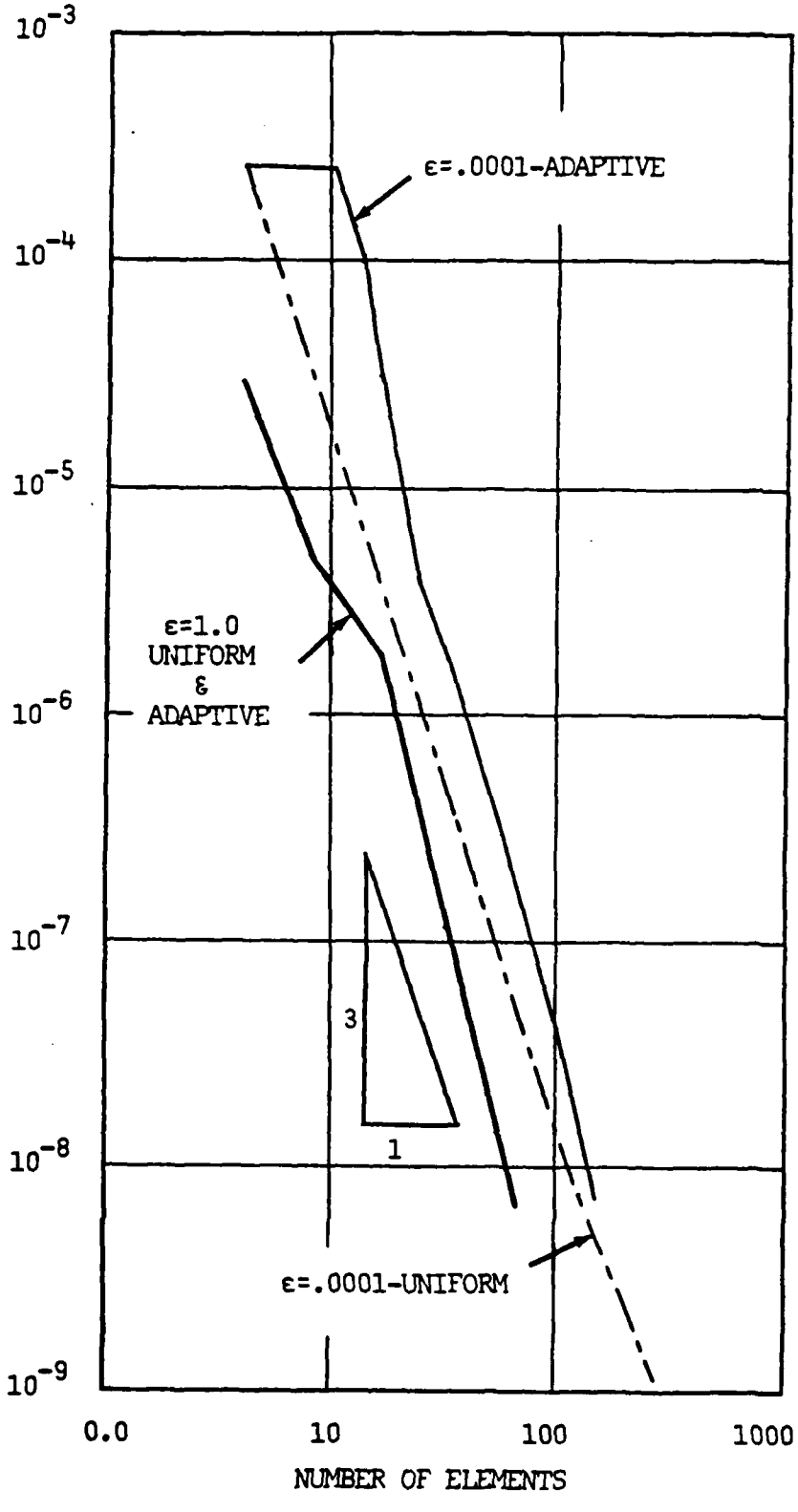

FIGURE 6: Maximum nodal errors for problem (4.1).

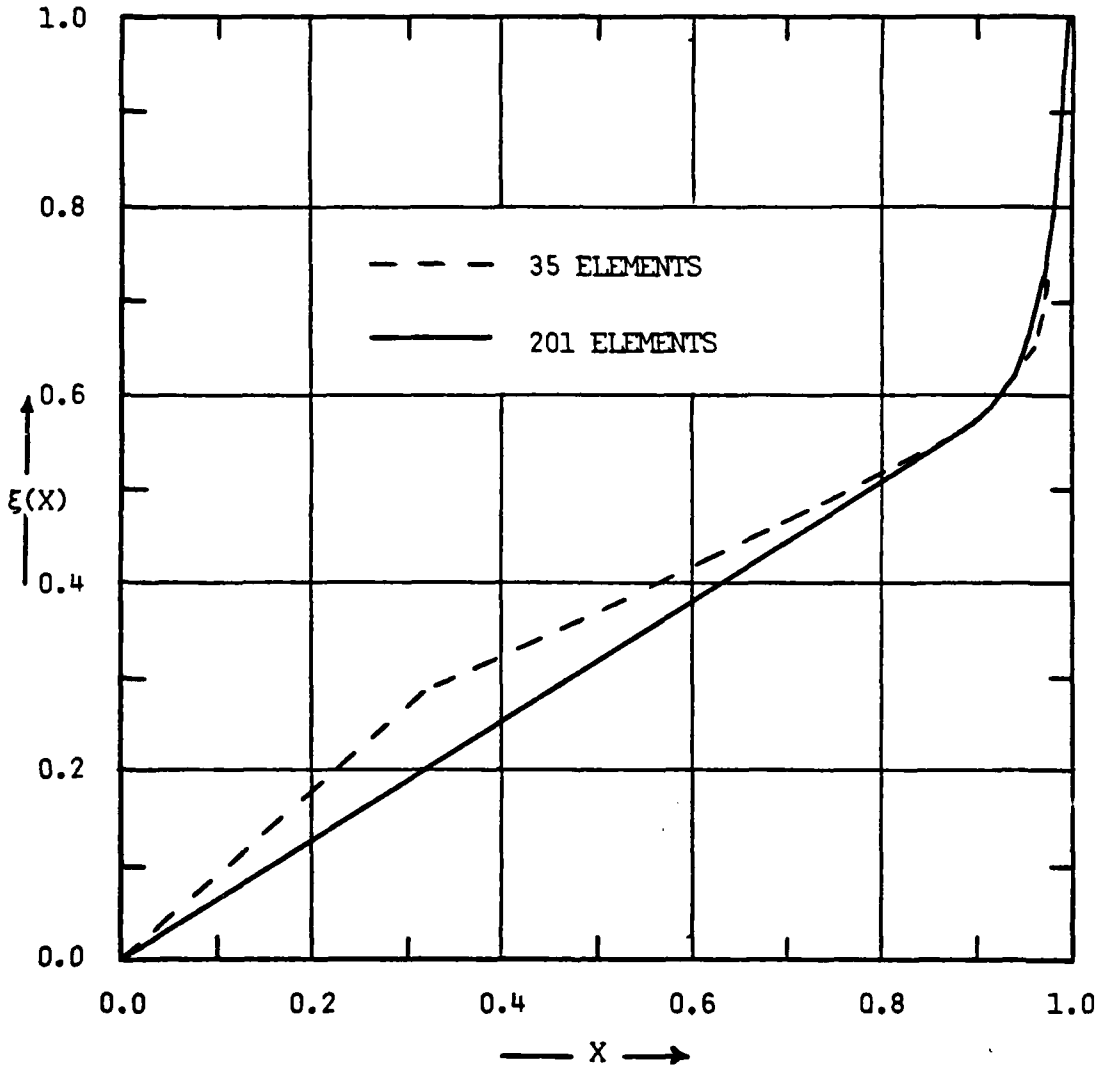

FIGURE 7: Mesh grading function for problem (4.1) when ε=.01.

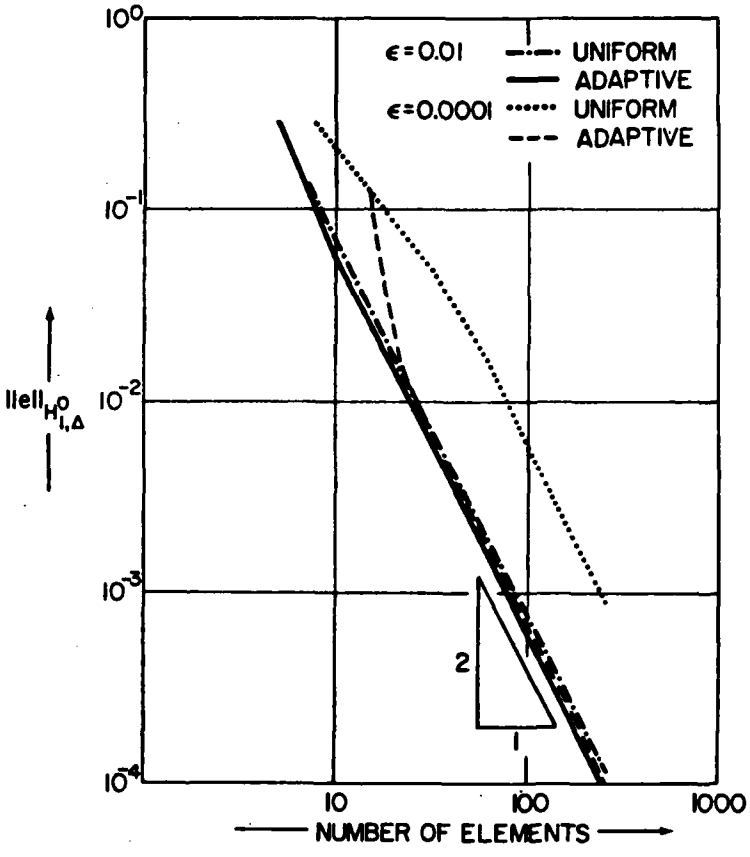

FIGURE 8: Errors in the $H^0_{1,\Delta}$ norm for problem (4.2).

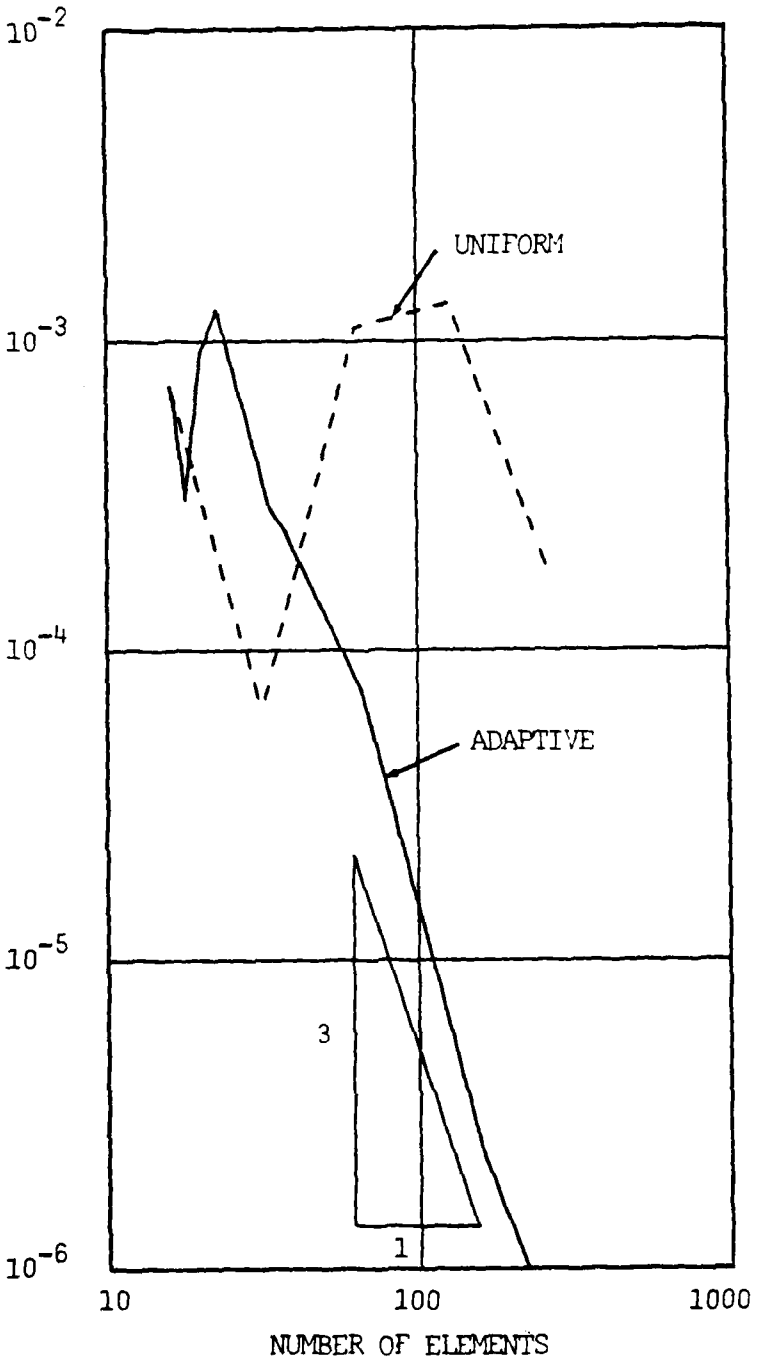

FIGURE 9: Maximum nodal errors for problem (4.2) when $\varepsilon = 10^{-4}$.

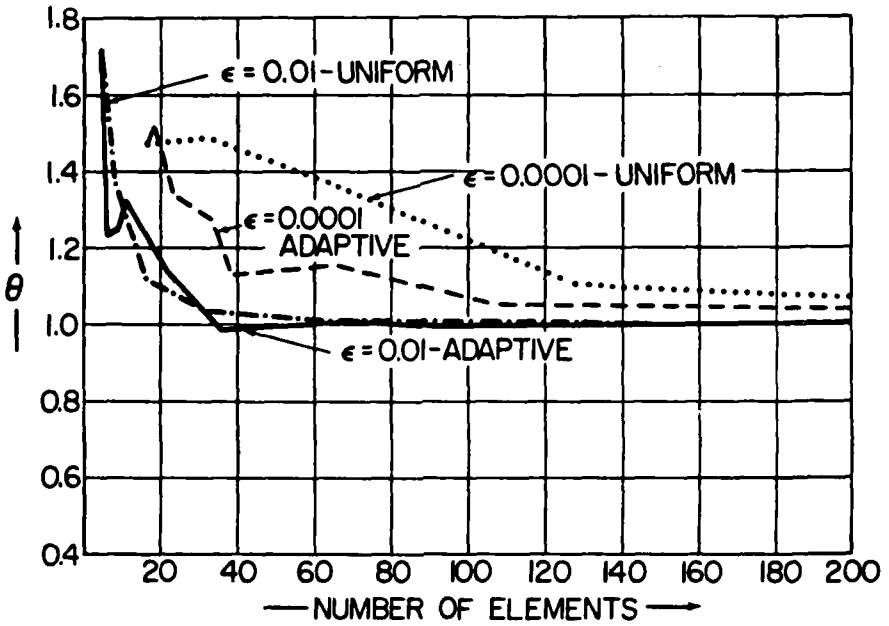

FIGURE 10: Effectivity indices for problem (4.2).

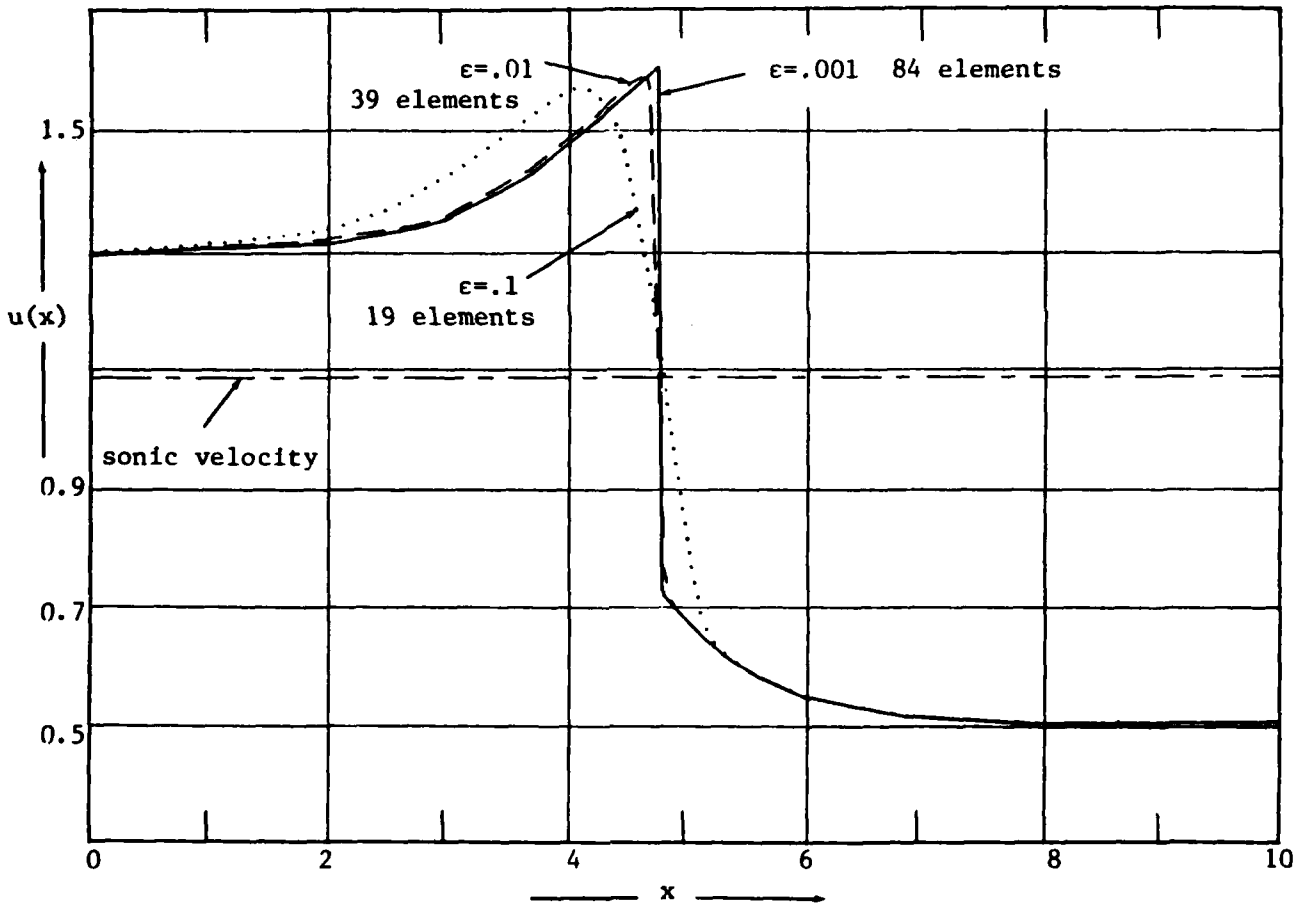

FIGURE 11: Computed solutions for the duct flow problem (4.3).

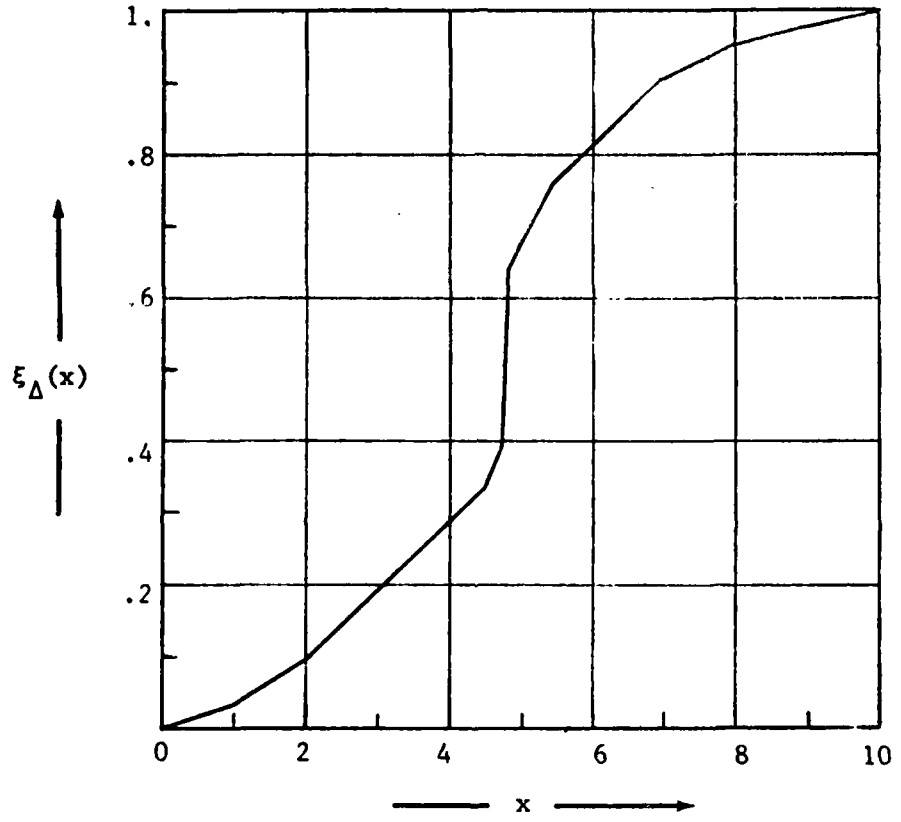

FIGURE 12: Mesh grading function for the duct flow problem with $\varepsilon = .001$ and 84 elements.

END

FILMED

6-83

DTIC